1982

Rolling Piston Type Rotary Compressor Performance Analysis

T. Matsuzaka

S. Nagatomo

ROLLING PISTON TYPE ROTARY COMPRESSOR

PERFORMANCE ANALYSIS

Takashi Matsuzaka
Shigemi Nagatomo

Toshiba Major Appliance Products Engineering Laboratory,
Kawasaki City, Japan

ABSTRACT

Analyses of loss factors which affect the rolling piston type rotary compressor efficiency have been theoretically and experimentally performed. Especially, it has been clarified that discharge port shape affects over-compression loss and re-expansion loss, and that mechanical loss can be significantly reduced by selecting the most suitable basic compressor dimensions.

Maximum compressor efficiency has been theoretically and experimentally evaluated, and it has been clarified that the efficience will be 74% on the basis of the recent highest engineering level regarding compressor design and manufacturing.
A highly-efficient compressor was produced base on the experiments, and has been tested. Compressor efficiency was 72.4%, comprising volumetric efficiency of 93%, compression efficiency of 94.8%, mechanical efficiency of 93.3% and motor efficiency of 88%.

INTRODUCTION

The features of the rolling piston type rotary compressor are high efficiency, low noise, high reliability, light weight, small-sized formation and others. Therefore, this type of compressor has been widely utilized for domestic air conditioners and refrigerating units recently, and this type of compressor satisfies the requirements of energy saving and conservation of resources which are present severe requirements.

Some research results have already been reported regarding this compressor (1) (2) (3) (4) (5), but synthetic performance research from the viewpoint of maximum compressor efficiency has not yet been performed.
The main objectives of this paper are as follows.
1. Primary loss factors will be recognized, and will be theoretically and quantitatively clarified.
2. The value of maximum compressor efficiency will be deduced on the basis of the present highest compressor design engineering.
3. A highly-efficient compressor will be produced by way of experiment, and will be tested.

The 3/4 horsepower, rolling piston type, high-pressure type rotary compressor was utilized for this research. Experiments were performed at 2,900 rpm and 3,500 rpm, but the maximum compressor efficiency is discussed based only on 2,900 rpm.

In this paper, the rolling piston type rotary compressor construction and features are explained, and thereafter, it is theoretically and experimentally shown that the optimum discharge port shape corresponds to maximum compressor efficiency, and that mechanical loss depends closely on the basic dimensions of the compressor components. Furthermore, the theoretical compressor efficiency and experimental performance of the highly-efficient compressor presently under trial production are shown.

DESCRIPTION OF THE ROTARY COMPRESSOR

1. Construction Features

The basic construction of the rotary compressor is shown in Fig. 1. The hermetic type rotary compressor, with the compression mechanism and the motor housed in the same shell, is widely utilized. The compression mechanism, with the cylinder in the center, is placed in the lower section, and a two-pole induction motor which drives the mechanism is placed in the upper

section, and these two are connected by a shaft. For lubrication of the compression mechanism, an appropriate amount of lubricating oil is sealed in the bottom section, which is completely sealed by a steel plate shell.

A roller is mounted on an eccentric shaft and rotates around the center of the cylinder. A suction pipe is directly inserted into the suction chamber, and high-temperature and high-pressure compression gas is discharged once into the shell internally through a discharge valve placed at an intermediate outlet of the discharge port.

2. Rotary Compressor Features

The basic features of the rotary compressor are discussed below.

A. High Efficiency Factor

As compression action and suction action are simultaneously conducted by one rotation of a roller ($\theta = 0° \sim 360°$), extremely smooth operation is performed. Moreover, as suction is continuous, a suction valve becomes unnecessary. Therefore, wire-drawing loss during suction periods and over-compression loss during discharge periods are extremely small, providing high compression efficiency.

B. High Volumetric Efficiency

As a suction pipe is directly connected to the cylinder suction port, suction gas superheat is almost eliminated, and a small specific volume of gas can be compressed in the cylinder. Also, based on the fact that there is no suction valve, smoothness of the suction process and the compression process and smaller top clearance volume formation based on the structural aspects, the volumetric efficiency of the rotary compressor is extremely high.

C. High Shell Internal Pressure

Based on sliding surface lubrication and compression gas sealing, the shell internal pressure is preserved at a high pressure, providing lubricating oil favorably to the respective mechanisms. Additionally, as the shell is on the high-pressure side, discharge gas containing oil droplets is discharged inside the shell once. Therefore, the shell functions as an oil separator, enabling favorable lubrication with a small amount of discharge oil from the compressor to the condenser.

D. Light Weight and Small-Sized Formation

As vibration in the rotary compressor is small, the motor and cylinder can be housed and held directly in the shell. Therefore, the main unit support member inside the shell can be eliminated. Additionally, the compression mechanism is extremely simple, and mufflers and similar components are almost completely eliminated, enabling utilization of a small number of components, as well as light weight and small-sized formation.

3. Efficiency and Loss Factor

Compressor efficiency is expressed by a coefficient of performance (COP), defined in relation to the refrigerating capacity and other non-dimensional efficiency factors. These factors are shown in Table 1.

EXPERIMENTAL AND THEORETICAL ANALYSES

1. Discharge Port Analysis

The shape of the discharge port is as shown in Fig. 2-(a). The port is placed near a blade, and is opened or closed by a discharge valve. Over-compression loss and re-expansion loss are caused by this discharge port.

A. Theoretical Analysis

Assumptions for simplifying analysis are as follows.
(1) Refrigerant is a perfect gas.
(2) Gas flow is isentropic.
(3) Pressure pulsation in the discharge manifold is negligible.
(4) Valve lift is constant.
(5) The discharge flow coefficient is constant.
(6) Angular rotation is constant.
A discharge port has two throats; that is, a port entrance throat and a valve seat throat. If it is assumed that density velocity through these two throats is equal to the compression gas velocity in the compressor, the following equation is obtained.

$$\rho_1 \cdot C_{D1} \cdot A_1 \cdot v_1 = \rho_2 \cdot C_{D2} \cdot A_2 \cdot v_2 = \rho_3 \cdot \frac{dVc}{dt} \quad (1)$$

Additionally, as it is considered that flow at the throat is isentropic, the following equations are obtained.

$$\frac{P_c}{P_i} = 1 + \frac{K}{2}\left(\frac{v_1}{a}\right)^2$$

$$\frac{P_i}{P_d} = 1 + \frac{K}{2}\left(\frac{v_2}{a}\right)^2 \quad (2)$$

By utilizing Eq. (1) and Eq. (2), the over-compression value is obtained by the following equation.

$$\frac{P_c - P_d}{P_d} = \frac{K}{2} S^2 \left(1 - \frac{R_r}{R_c}\cos\theta\right) \quad (3)$$

where

$$S = \frac{N \cdot V_{st}}{60 \cdot A_{eff} \cdot a}$$

$$\frac{1}{A_{eff}^2} = \frac{1}{(C_{D1} \cdot A_1)^2} + \frac{1}{(C_{D2} \cdot A_2)^2} \quad (4)$$

Over-compression loss W_o is obtained by integrating Eq. 3.

$$\frac{W_o}{P_d \cdot V_{st}} = \frac{K}{4} S^2 \left[\left\{1 + \frac{3}{2}\left(\frac{R_r}{R_c}\right)^2\right\}(2\pi - \theta_d) + \left\{3\left(\frac{R_r}{R_c}\right) + \frac{3}{4}\left(\frac{R_r}{R_c}\right)^3\right\}\sin\theta_d - \frac{3}{4}\left(\frac{R_r}{R_c}\right)^2 \sin 2\theta_d + \frac{1}{12}\left(\frac{R_r}{R_c}\right)^3 \sin\theta_d \right] \quad (5)$$

The following assumptions are set for obtaining the relative equation between the top clearance volume V_{cp} and re-expansion loss.
(1) Re-expansion gas flows entirely into the compressor cylinder, and does not counterflow to the suction port.
(2) Re-expansion gas timing is at the upper dead point.
Pressure increase ΔP caused by flowing residual gas into the cylinder is expressed by the following equation.

$$\Delta P = K P_s \left(\frac{P_d}{P_s}\right)^{\frac{1}{K}} \cdot \left(\frac{V_{cp}}{V_{st}}\right) \quad (6)$$

As a result, the compression chamber pressure P_s' at the start of compression is as follows.

$$P_s' = \left\{1 + K\left(\frac{P_d}{P_s}\right)^{\frac{1}{K}} \cdot \frac{V_{cp}}{V_{st}}\right\} P_s \quad (7)$$

Adiabatic work L_{ad}' is obtained by the following equation.

$$Lad' = \frac{K}{K-1} P_s' V_{st} \left\{\left(\frac{P_d}{P_s'}\right)^{\frac{K-1}{K}} - 1\right\} + V_{st} \cdot \Delta P \quad (8)$$

Re-expansion loss W_R is calculated by subtracting the non-top clearance volume adiabatic work L_{ad} from L_{ad}'.

$$W_R = L_{ad}' - L_{ad} \quad (9)$$

Meanwhile, when re-expansion gas flows into the cylinder, the suction process has almost ended. Therefore, suction gas flow is not affected by residual gas re-expansion, and, as a result, the compressor can maintain a constant refrigerating capacity.

B. Experimental Analysis

For the experiments, a rolling piston type rotary compressor with a stroke volume of 9.35 cc/rev. was utilized. Compressor power consumption and refrigerating capacity were measured by a secondary refrigerant calorimeter. Pressures in the cylinder and the suction chamber were measured with piezo type pressure transducers mounted on the cylinder wall near the discharge port and the suction port, respectively [Fig. 2-(a), Fig. 2-(b)]. Discharge valve behavior was measured with two gap sensors mounted on the valve stopper. Rotation timing of the compressor was also measured with a gap sensor.

The experiments were performed on various discharge port radii.
The test conditions were as follows.
Discharge pressure: 2.16 Mpa
Suction pressure: 0.63 Mpa
Rotation number: 2,900 rpm and 3,500 rpm

The P-V diagram gained by cylinder pressure measured with two pressure transducers is shown in Fig. 3-(a) and Fig. 3-(b) and the pressure variation, valve behavior and rotation timing during one rotation are shown in Fig. 4. In Fig. 4, cylinder pressure and discharge pressure are the same value at point A, and the cylinder pressure indicates the maximum value at point B. Point C shows the timing where over-compression is almost zero, and the discharge valve is not yet closed. At point D, the discharge valve is almost closed, and re-expansion of residual gas has already started.

Re-expansion is completed at point E, and suction pressure affected by re-expansion is rapidly increasing at an angular displacement of 360°. Experimental over-compression and wire-drawing losses via various discharge port diameters are shown in Fig. 5, and volumetric efficiency (η_v) and overall mechanical efficiency (η_{meo}) are shown in Fig. 6. The following clarifications were obtained by these experimental analyses.
(1) Over-compression loss decreases as a consequence of discharge port diameter increase.
(2) Wire-drawing loss has no relationship to discharge port diameter.

(3) Volumetric efficiency is not affected by discharge port diameter, and is maintained at a constant value.
(4) There is a maximum overall mechanical efficiency, depending upon the most suitable discharge port diameter.

C. Results

As it is clarified that there is no counterflow of re-expansion gas into the suction port by experimental analysis, and that the flow timing is almost at the upper dead point, assumptions for obtaining the calculation equation are considered to be sufficient. Over-compression loss, re-expansion loss and discharge port loss are shown in Fig. 7, in which the horizontal axis is the discharge port diameter.

The calculation results were compared with the experimental values regarding over-compression loss. The results meet the experimental values relatively well.
By selecting the most suitable discharge port radius, discharge port loss can be reduced.

2. Mechanical Loss Analysis

The following six losses are considered as mechanical loss.
(1) Crankshaft bearing loss $W_{c\ell}$
(2) Main bearing loss $W_{m\ell}$
(3) Sub-bearing loss $W_{s\ell}$
(4) Blade bearing loss $W_{b\ell}$
(5) Thrust bearing loss $W_{t\ell}$
(6) Rotor windage loss $W_{w\ell}$
Blade tip friction loss, roller surface friction loss and oil pump loss are omitted, because of the small values when compared to the aforementioned losses.

A. Calculation Method

Journal Bearing Loss

The main bearing, sub-bearing and crankshaft bearing are typical journal bearings, and these losses were obtained, utilizing the journal bearing fundamental equation, when static load is applied.

$$\frac{\partial}{\partial x}\left(\frac{h^3}{6\eta}\cdot\frac{\partial P}{\partial x}\right)+\frac{\partial}{\partial z}\left(\frac{h^3}{6\eta}\cdot\frac{\partial P}{\partial z}\right)=U\frac{\partial h}{\partial x} \tag{11}$$

As rotary compressor bearing dimensions are usually in the range of $4 > L/D > 0.25$, Eq. (11) can only be solved by the numerical analysis method, providing for bearing loss thereby.

Friction force F_{jf} is obtained as follows.

$$F_{jf} = K_f\cdot(C/D)\cdot F \tag{12}$$

where F is the shaft load and C is the diameter clearance.

Crankshaft loading force $|F_{cr}$ is the sum of gas force $|F_{cg}$, roller centrifugal force $|F_{rc}$, blade tip force $|F_{br}$ (composed of spring force $|F_{bs}$ and gas force $|F_{bp}$) and blade inertia $|F_{bi}$, as shown in Fig. 8.

$$|F_{cr} = |F_{cg} + |F_{rc} + |F_{br} + |F_{bi} \tag{13}$$

Meanwhile, main bearing force $|F_m$ and sub-bearing force $|F_s$ are obtained as shown in the following equation.

$$|F_m = |F_s = \frac{1}{2}|F_{cr} \tag{14}$$

Blade Slot Loss

If it is assumed that the pressure on the high-pressure side blade surface is equal to that of the low-pressure side blade surface in a blade slot, the gas pressure force model on the blade is as shown in Fig. 9. The blade tip inserted into the cylinder is pushed in the direction of the low-pressure side by the pressure difference between the compression chamber pressure P_c and suction pressure P_s. If the force caused by the pressure difference is loaded on the blade as a concentrated load, there is no blade deformation and the oil viscosity force in the blade slot clearance is negligible, blade force F_b is as follows.

$$F_b = \left(1+\frac{Y_b}{L_b}\right)F_{bg}$$
$$F_{bg} = Y_b(\theta)\cdot H_{b\ell}\cdot(P_c(\theta) - P_s) \tag{15}$$

where,
F_{bg}; Pressure difference force,
$Y_{b(\theta)}$; Blade displacement,
$H_{b\ell}$; Blade height, and
$P_{c(\theta)}$; Cylinder pressure.
Therefore, blade friction force F_{bf} is obtained.

$$F_{bf} = \mu_b\cdot F_b \tag{16}$$

Thrust Bearing Loss

The thrust bearing lubrication condition seems to be boundary, but it is not clear. In this paper, Coulomb friction force is considered.

$$F_{tf} = \mu_t(w_{sh} + w_{Ro}) \tag{17}$$

Motor Rotor Windage Loss

As the balance weight is mounted on the end of the motor rotor, drag force F_{rd} caused by the projected sectional area of

the balance weight is generated.

$$F_{rd} = C_d \cdot \frac{1}{2} \cdot \rho \cdot V^2 \cdot A_r \quad (18)$$

where,
C_d; Drag coefficient,
ρ; Gas density,
V; Rotor velocity, and
A_r; Balance weight sectional area

B. Calculation Results

Theoretical gas forces and friction losses are shown in Fig. 10 and Fig. 11.
The basic dimensions and calculated friction losses are shown in Table 2 and 3. From these calculation results, it is clarified that each friction loss can be significantly changed by selecting the basic dimensions.

C. Comparison of Theory and Experiments

Theoretical and experimental friction losses are compared in Table 4. Total friction loss $W_{f\ell}$ can be calculated by utilizing the measured motor efficiency and the P-V diagram.

$$W_{f\ell} = \eta_{mo} \cdot W - \oint PdV \quad (19)$$

The theoretical values match the experimental values relatively well.

MAXIMUM COMPRESSOR EFFICIENCY

Maximum compressor efficiency can be obtained by minimizing all of the compressor losses.
For this purpose, volumetric efficiency, compression efficiency, mechanical efficiency and motor efficiency should be the maximum values.

Volumetric Efficiency

Volumetric loss is made up of suction loss, gas superheat loss and leakage loss, but gas superheat loss and suction loss are less than leakage loss.
As leakage loss is affected by the blade and roller clearances, oil viscosity and refrigerant solubility into oil and other factors, it is difficult to calculate these losses by utilizing a theoretical equation.
According to our various tests results in regard to clearance and oil viscosity, maximum volumetric efficiency was approximately 94% at 2,900 rpm.

Compression Efficiency

Compression loss is made up of wire-drawing loss, over-compression loss and re-expansion loss.
The minimum values of these losses are assumed from Fig. 7 as follows. Wire-drawing loss, over-compression loss and re-expansion loss are approximately 1.0%, 1.5% and 1.5%, respectively. Therefore, the synthetic maximum compression efficiency is approximately 96%.

Mechanical Efficiency

In the case of improving the mechanical efficiency, it is required to consider lubrication, reliability and vibration.
As lubrication conditions must be assumed when calculating mechanical loss, error in calculation accuracy is inevitable, within 2%.
The calculated maximum mechanical efficiency was approximately 94%.

Motor Efficiency

Motor efficiency can be increased by decreasing the copper loss and the iron loss.
The efficiency of the motor utilized for the rotary compressor is approximately 80% to 85%, but in the near future, it will be possible to produce a motor with an efficiency of approximately 88%.

Maximum Compressor Efficiency

Maximum compressor efficiency via motor efficiency is shown in Fig. 12. Maximum compressor efficiency is 74% at the point of 88% motor efficiency.
Therefore, the maximum COP is 353%.

TRIAL PRODUCTION OF HIGHLY-EFFICIENT COMPRESSOR

A highly-efficient compressor, investigating the leakage loss, optimum discharge port and minimum mechanical loss, has been produced by way of experiment.
A two-pole induction motor, for which the efficiency is 88%, was mounted.
The measured performance under the test conditions shown in Table 5 is shown in Table 6.
The compressor efficiency was obtained from these performances.
Variation loss rates are shown in Table 7 regarding the original compressor (before) and the improved compressor (after).
The measured compressor efficiency approaches the theoretical maximum compressor efficiency of 74%.

CONCLUSION

1. The maximum compressor efficiency of 74% was theoretically and experimentally obtained.

2. Synthetic efficiency of 72.4% for the compressor was obtained during trial production. The efficiency was composed of volumetric efficiency of 93%, compression efficiency of 94.8%, mechanical efficiency of 93.3% and motor efficiency of 88%.

3. The discharge port affects over-compression loss and re-expansion loss. There is a most suitable shape for obtaining the maximum compression efficiency.

4. Over-compression loss, re-expansion loss and valve behavior were clarified by experiments.

5. The relationship between the basic compressor dimensions and mechanical loss was clarified quantitatively. The bearing dimensions especially affect the mechanical loss.

NOMENCLATURE

A	Area
A_{eff}	Effective flow area
A_r	Motor balance sectional area
a	Sound velocity
C	Diameter clearance
C_D	Discharge coefficient
C_d	Drag coefficient
D	Diameter
h	Oil film thickness
F	Force
K_f	Friction force coefficient
K	Specific ratio
L	Journal bearing length
L_b	Blade length in slot
Y_b	Blade displacement
N	Rotation number
Lad	Adiabatic work
P	Pressure
P_d	Discharge pressure
P_s	Suction pressure
P_i	Port pressure
S	Discharge flow constant
t	Time
U	Circumference velocity
v	Gas velocity
V_{st}	Stroke volume
V_{cp}	Top clearance volume
V_c	Compression volume
W	Compressor power consumption
W_o	Over-compression loss
W_R	Re-expansion loss
$W_{c\ell}$	Crankshaft bearing loss
$W_{m\ell}$	Main bearing loss
$W_{s\ell}$	Sub bearing loss
$W_{t\ell}$	Thrust bearing loss
$W_{w\ell}$	Motor rotor windage loss
$W_{f\ell}$	Total friction loss
w_{sh}	Shaft weight
w_{Ro}	Motor rotor weight
η	Viscosity coefficient
η_{me}	Mechanical efficiency
η_{mo}	Motor efficiecy
η_c	Compression efficiency
η_{comp}	Compressor efficiency
η_v	Volumetric efficiency
η_{meo}	Overall mechanical efficiency ($\eta_{meo} = \eta_v \cdot \eta_c \cdot \eta_{me}$)
μ	Friction coefficient
ρ	Density
θ	Rotation angular

REFERENCES

(1) 1978, P. Pandeya, Rolling Piston Type Rotary Compressors with Special Attention to Friction and Leakage.

(2) 1978, Itsuo Chu, Analysis of The Rolling Piston Type Rotary Compressor.

(3) 1980, S. Nagatomo, Estimation of The Starting Torque of Refrigerant Rotary Compressor.

(4) 1980, M. Ozu, Some Electrical Observation of Metallic Contact Between Lubricated Surfaces Under Dynamic Conditions Rotary Compressor.

(5) 1980, H. Tanaka, Noise and Efficiency of Rolling Piston Type Refrigeration Compressor for Household Refrigerator and Freezer.

Note: All references are from Purdue Compressor Technology Conference Proceedings.

Helen Glick
Conference Secretary

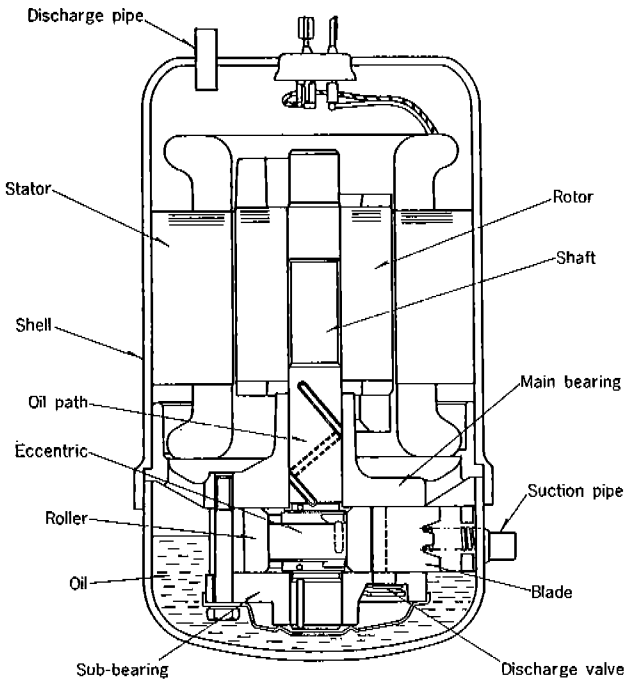

Fig. 1 Rotary compressor construction

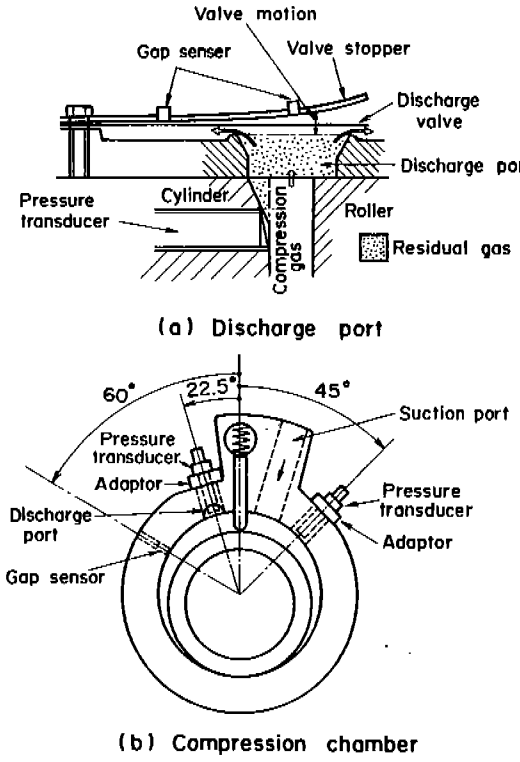

Fig. 2 Transducer mounting

Table 1 Efficiency and loss Factor classification

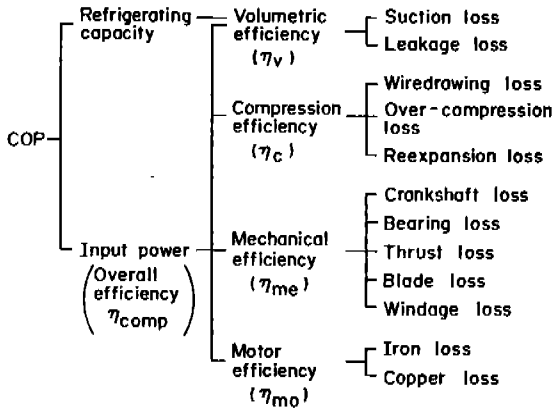

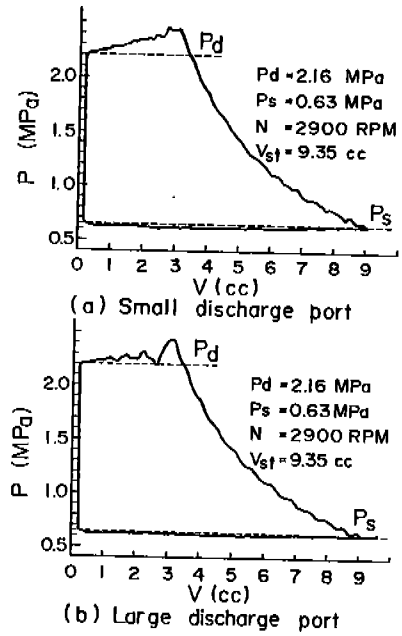

Fig. 3 Measured P-V diagram

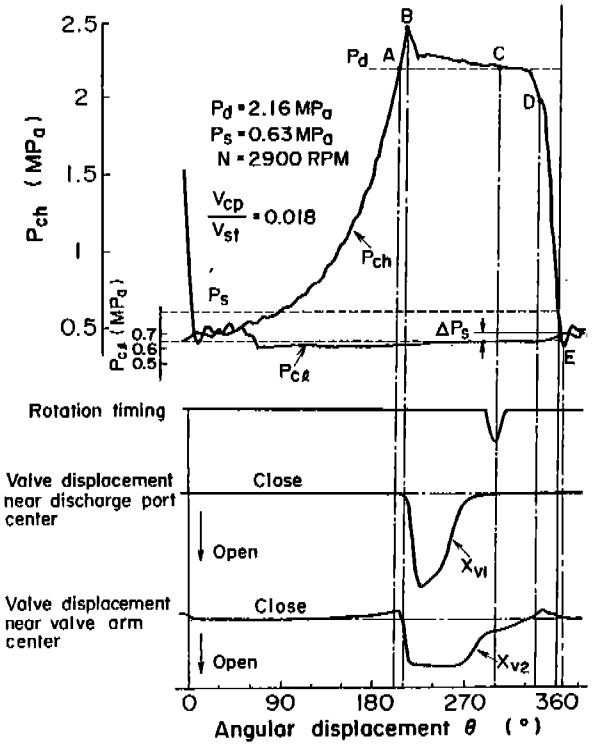

Fig. 4 Pressure variation and valve behavior

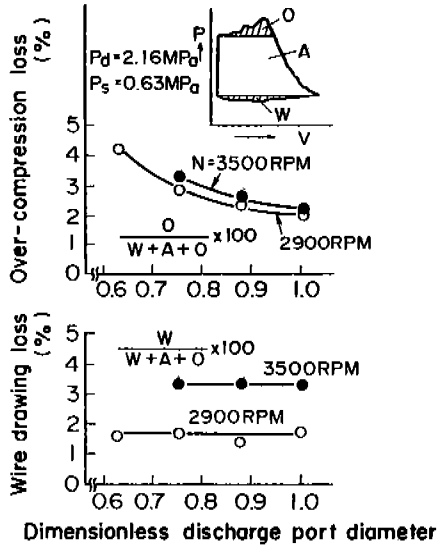

Fig. 5 Discharge port diameter effects on over-compression and wiredrawing loss

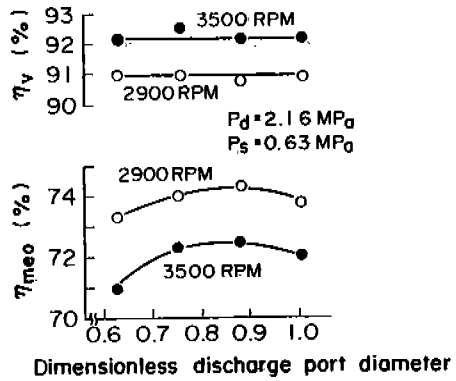

Fig. 6 Discharge port diameter effects on volumetric efficiency and overall mechanical efficiency

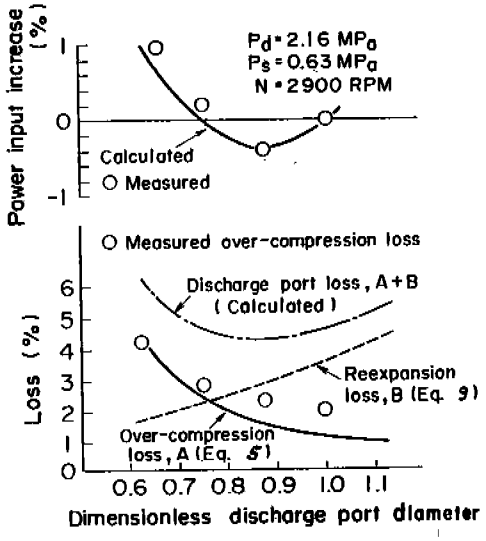

Fig. 7 Comparison of measured and calculated values of discharge port loss

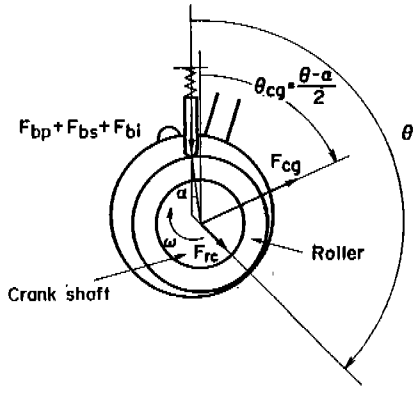

Fig. 8 Force on crankshaft

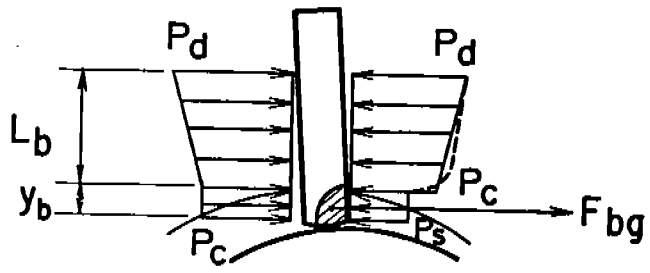

Fig. 9 Gas pressure force on blade

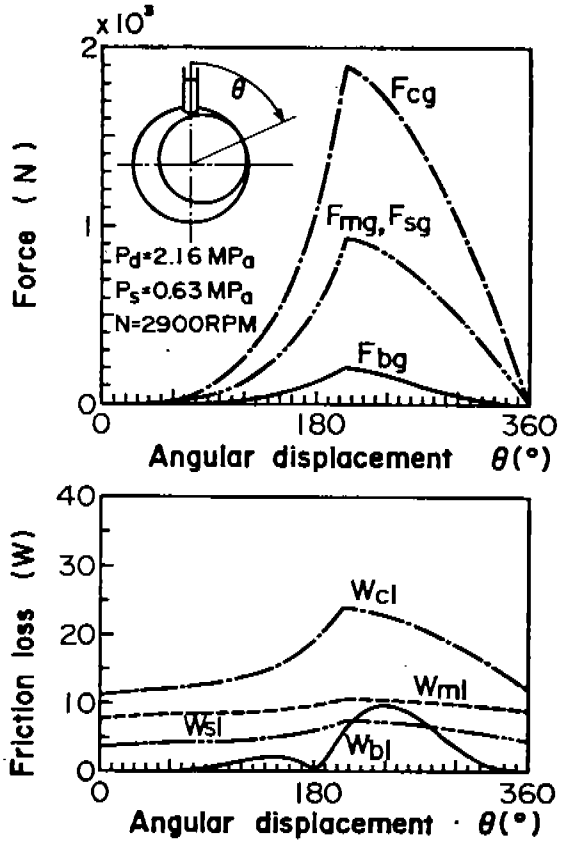

Fig. 10 Force and friction loss for basic dimension BD1

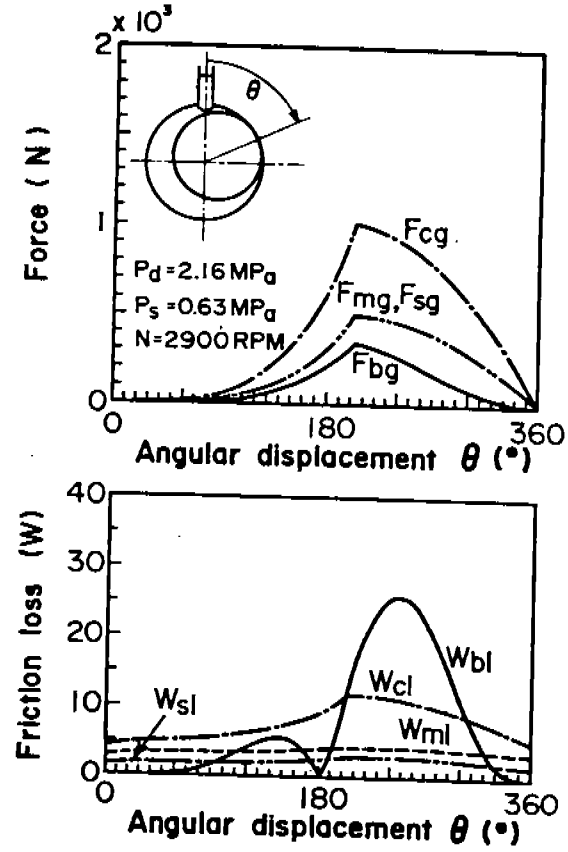

Fig. 11 Force and friction loss for basic dimension BD2

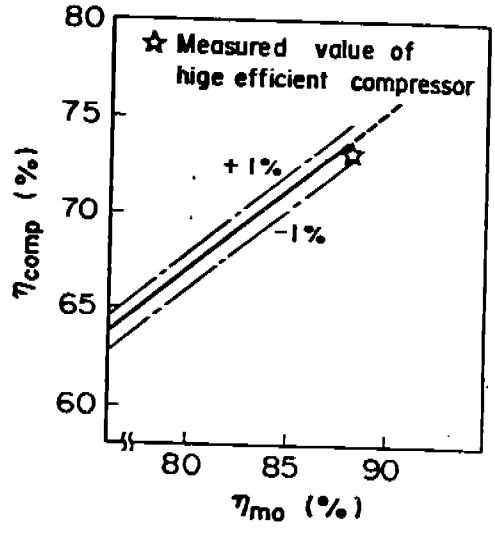

Fig. 12 Calculated and measured maximum overall efficiency

Table 2 Basic dimension values

Basic dimension		BD 1	BD 2
Displacement volume	V_{st}	1	1
Cylinder radius	R_{cyl}	1	0.76
Roller radius	R_{ro}	1	0.67
Cylinder height	H_{cyl}	1	0.80
Blade width	B	1	0.79
Blade bearing length	L_b	1	1
Top clearance volume	V_{cp}	1	0.5
Crank shaft diameter	D_{cr}	1	0.80
Crank shaft length	L_{cr}	1	0.75
Main bearing diameter	D_m	1	0.80
Main bearing length	L_m	1	0.63
Sub bearing diameter	D_s	1	0.75
Sub bearing length	L_s	1	0.75
Rotar balance area	A_r	1	0.5

Table 3 Calculated friction loss

(W)

Revolution	3500 RPM		2900 RPM	
Basic dimension	BD 1	BD2	BD 1	BD2
W_{cr}	21.7	9.9	15.7	7.3
W_m	12.2	5.0	8.6	3.5
W_s	7.1	3.0	5.1	2.2
W_b	3.2	8.7	2.6	7.3
W_t	9.1	7.3	7.5	6.0
W_w	12.0	6.0	8.3	4.2
W_{total}	65.3	39.9	47.8	30.5

Table 4 Friction loss comparison of theory and experiment

Revolution	Dimension	Theory	Experiment
2900 RPM	BD 1	47.8 W	53 W
	BD 2	30.5 W	31 W
3500 RPM	BD 1	65.3 W	66 W
	BD 2	39.9 W	41 W

Table 5 Testing condition

P_s : 0.63 MPa
T_s : 308.15 K
P_d : 2.16 MPa
100 V 50 Hz 2900 RPM
Compressor out put 3/4 H_P
Refrigerant R-22

Table 6 Measured performance

Overall efficiency	72.4 %
Volumetric efficiency	93.0 %
Compression efficiency	94.8 %
Mechanical efficiency	93.3 %
Motor efficiency	88.0 %

Table 7 Consumption power before and after performance improvement

	After	Before
Isentropic work	72.4 %	61.7 %
Leakage loss	5.1 %	5.7 %
Wiredrawing loss	1.1 %	1.3 %
Over-compression loss	1.7 %	1.5 %
Reexpansion loss	1.5 %	4.3 %
Crankshaft loss	1.6 %	2.8 %
Journal bearing loss	1.2 %	2.4 %
Thrust bearing loss	1.3 %	1.4 %
Blade loss	1.6 %	0.5 %
Windage loss	0.4 %	1.4 %
Motor loss	12.0 %	16.0 %
Unknown loss	0.1 %	1.0 %
TOTAL	100.0 %	100.0 %